



LAWRENCE
LIVERMORE
NATIONAL
LABORATORY

Geometrical Considerations for Piezoresistive Microcantilever Response to Surface Stress during Chemical Sensing

A. Loui, F.T. Goericke, T.V. Ratto, J. Lee, B.R.
Hart, W.P. King

May 2, 2008

Sensors and Actuators A: Physical

Disclaimer

This document was prepared as an account of work sponsored by an agency of the United States government. Neither the United States government nor Lawrence Livermore National Security, LLC, nor any of their employees makes any warranty, expressed or implied, or assumes any legal liability or responsibility for the accuracy, completeness, or usefulness of any information, apparatus, product, or process disclosed, or represents that its use would not infringe privately owned rights. Reference herein to any specific commercial product, process, or service by trade name, trademark, manufacturer, or otherwise does not necessarily constitute or imply its endorsement, recommendation, or favoring by the United States government or Lawrence Livermore National Security, LLC. The views and opinions of authors expressed herein do not necessarily state or reflect those of the United States government or Lawrence Livermore National Security, LLC, and shall not be used for advertising or product endorsement purposes.

Geometrical Considerations for Piezoresistive Microcantilever Response to Surface Stress during Chemical Sensing

A. Loui,^a F.T. Goericke,^b T.V. Ratto,^a J.Lee,^b B.R. Hart,^a and W.P. King^{b*}

^a*Lawrence Livermore National Laboratory, 7000 East Ave., Livermore, CA 94550, USA*

^b*Department of Mechanical Science and Engineering, University of Illinois at Urbana-Champaign,
Urbana, IL 61822*

*To whom correspondence should be addressed: Phone: 217-244-3864; Email: wpk@uiuc.edu

ABSTRACT

We have designed, fabricated, and tested five piezoresistive cantilever configurations to investigate the effect of shape and piezoresistor placement on the sensitivity of microcantilevers under either point loading and surface stress loading. The experimental study reveals that: 1) high aspect ratio cantilevers that are much longer than they are wide are optimal for point-loading applications such as microscopy and force measurements; 2) low aspect ratio cantilevers that are short and wide are optimal for surface stress loading scenarios such as those that occur in biological and chemical sensor applications. The sensitivity data for both point loads and surface stress are consistent with previously developed finite-element models.

Keywords: cantilever sensor, piezoresistor, atomic force microscopy, chemical sensing, surface stress

1. Introduction

Microcantilevers are highly sensitive transducers for a variety of physical phenomena. In particular they are sensitive to applied stress [1-3]. For soft cantilevers, such as those employed in atomic force microscopy, the bending sensitivity can approach a few tenths of a newton per meter. For this reason, these miniaturized structures have been widely studied as transducers for biological and chemical sensors [4-7]. In the latter case, a coating is typically applied to one side of the cantilever that, in the presence of some chemical species, undergoes volumetric expansion or contraction; if this functional layer is well-adhered to the substrate, the microcantilever will deform.

Microcantilever deflection is most commonly measured by reflecting a laser from the free end of the cantilever. However the need for a laser and external optics is obviated if a piezoresistive strain sensor is integrated into the cantilever [8]; in this case, the applied surface stresses are measured directly, with the mechanical energy transduced into a readily measurable electrical signal. Much research has focused on the design, fabrication, and optimization of these types of cantilevers [9-11]. Recently, simulations have shown that piezoresistive cantilevers designed for atomic force microscopy (AFM) may not be optimal for biochemical sensing [12]. The main difference between these two cases is that an AFM cantilever experiences a point load at its free end (where the probe tip is located), whereas a cantilever with a functional coating for sensing applications experiences a distributed surface stress. The mechanical strain that occurs in cantilevers under these two types of usage, and the corresponding spatial maps of stress difference (lateral minus transverse), are compared in Fig. 1.

Contrasting patterns of internal stress difference across a cantilever are observed for point versus surface mechanical loading. The key physical parameter for inducing a change in the resistance of a piezoresistor is not absolute stress or strain, but rather the difference between lateral stress and transverse stress in the cantilever, which can be denoted as $\sigma_{lt}=\sigma_l-\sigma_t$. In the case where a surface stress is applied to the cantilever, as occurs during biological and chemical sensing, the stress difference has its largest magnitude in the central region near the base of the cantilever. The fractional change in resistance of a piezoresistive cantilever under mechanical load is proportional to σ_{lt} ; therefore, the precise placement of the piezoresistor within this region of maximum σ_{lt} is crucial for optimizing sensitivity to applied surface stresses and hence, to sensing applications where such applied stresses occur.

In this paper, we describe the design, fabrication, and testing of five piezoresistive cantilever configurations for biological and chemical sensing applications. These five designs offer the ability to test the effect of shape and piezoresistor placement on the piezoresistive sensitivity under surface mechanical loading. We also subject the cantilevers to experimental validation under actual conditions of chemical sensing, using the hydrogen/palladium interaction as a representative sensing system.

2. Cantilever design and fabrication

For boron doped (p-type) piezoresistors in single-crystal silicon, the lateral and transverse piezoresistive coefficients are of comparable magnitude but of opposite sign [13]. The highest piezoresistor signal output occurs when the difference between the lateral and transverse stresses within the cantilever is maximized [12]. In atomic force

microscopy, the stress difference is distributed along the length of the cantilever, while for sensing applications, the stress difference is localized the cantilever base (Fig. 1). Generalized design conclusions are published elsewhere [12], but can be summarized as follows: cantilevers designed as transducers for sensors should be short and wide rather than long and narrow, in order to derive maximum benefit from the localization of high stress difference near the cantilever base during the application of surface stress.

To experimentally test these predictions, five types of microcantilevers with different shapes and piezoresistor regions were designed to study the effect of geometrical parameters on the sensitivity to surface stress. Figure 2 shows a schematic of these cantilevers, in which light-shaded areas indicate the boron-doped (piezoresistive) regions, and dark-shaded areas indicate intrinsic (insulating or highly resistive) regions. A cantilever length of $L_c = 200 \mu\text{m}$ was selected for all five designs. Type A has a low length to width ratio (LWR or aspect ratio) of unity, and is expected to be highly sensitive to surface stress loading. The piezoresistive element was placed in the center of the clamped cantilever base, where the highest stress difference (lateral minus transverse) is located during surface stress loading; under such conditions, the largest change in overall resistance will result. The piezoresistor defines a U-shaped region that extends $60 \mu\text{m}$ into the cantilever from its base (Fig. 2a). The lateral extent of this current flow path was selected to ensure that the bulk of the piezoresistor lies within the free-standing portion of the microcantilever; this value is compatible with the typical sidewall profiles produced by deep reactive-ion etching (DRIE). For the purposes of easy visual identification and geometric convenience, we will refer to the lateral extent of the

piezoresistor as the “piezoresistor length” L_p ; note that the actual piezoresistor length is more than two times this value.

Since the overall shape and piezoresistor length vary amongst the five designs, it is useful to define a fractional piezoresistor length as the ratio of the nominal piezoresistor length to the overall length of the cantilever: L_p/L_c . By this definition, cantilever type A has a fractional piezoresistor length of 0.3 (Fig. 2a).

Type C was designed to increase the base width while keeping the surface area, and piezoresistor placement and length, the same as for type A. The resulting shape is a trapezoid with an angle of 60° between the base width and transverse edges (Fig. 2c). Types B and D have the same overall geometries as types A and C, respectively, but are boron-doped across their entire surface area and therefore possess longer, proportionate piezoresistors (Figs. 2b, 2d). The results of a recent theoretical study suggest that these two designs (with $L_p/L_c = 1.0$) should have less sensitivity to surface stress than their respective counterparts (with $L_p/L_c = 0.3$) [12]. Cantilever type E possesses a LWR of two and, like types B and D, is boron-doped over its entire surface area; this design is consistent with conventional AFM-type cantilevers, and is included in this study for comparative purposes.

The fabrication process for these five cantilever designs was adopted from Refs. [14, 15], and is schematically illustrated in Fig. 3. The fabrication process starts with an n-type silicon-on-insulator (SOI) wafer of orientation $\langle 100 \rangle$, where the silicon device layer is $2 \mu\text{m}$ thick, the buried oxide (BOX) layer is $1 \mu\text{m}$ thick, and the silicon handle layer is $400 \mu\text{m}$ in thickness. After thinning of the device layer to the target thickness (*ca.* $1 \mu\text{m}$) by thermal oxidation and grown oxide etching, the cantilever structures are

patterned with a photoresist and etched into the silicon device layer using a Bosch process in an inductively coupled plasma (ICP) etcher (Fig. 3a). To define the piezoresistors, boron is selectively implanted at a dose and kinetic energy of $2 \times 10^{14} \text{ cm}^{-2}$ and 30 keV, respectively, with hard-baked positive photoresist as a mask (Fig. 3b). Then the photoresist mask is removed, and a 200 nm thick layer of silicon dioxide is deposited using plasma enhanced chemical vapor deposition (PECVD) to prevent the dopant from diffusing out of the silicon into the ambient during the subsequent heat treatment. The heat treatment is performed in a rapid thermal processing tool to activate the dopant while minimizing its redistribution via diffusion. After heat treatment, the contacts connecting the doped silicon to the metal layer are defined with the ICP etcher, and aluminum metallization is performed using electron beam deposition in combination with a liftoff process (Fig. 3c). The processed wafer is sintered at 400 °C in a forming gas for 30 minutes to allow interdiffusion of the doped silicon and aluminum; this step produces the junctions between the piezoresistor and the external electrodes. Finally, the handle layer is etched from the backside using the Bosch process in the ICP etcher (Fig. 3d), and the excess portions of the BOX layer are removed with 49 wt% hydrofluoric acid solution (Fig. 3e). Figure 4 shows scanning electron micrographs of the released devices; although only single, representative cantilevers are shown, each design type was fabricated in adjacent pairs on a silicon chip to allow differential measurements to be performed during the experimental validation studies.

3. Cantilever Characterization

The microcantilevers were tested under both the point and surface mechanical loading. For the point load test, each cantilever was mounted, wired into a Wheatstone bridge circuit, and probed with a closed-loop micropositioner. We have used this approach to measure point load deflection sensitivity in previous reports [14, 16] and do not discuss the technique in further detail here. Figure 5 shows the cantilever piezoresistor response to a tip deflection. Cantilever type E, with an aspect ratio consistent with AFM-type cantilevers, has a point-load sensitivity that is approximately 4.4 times greater than the square type B cantilever, despite both designs having similarly shaped piezoresistors.

The trapezoidal geometries (types C and D) exhibit sensitivities to point-loading that are similar to their square-shaped counterparts (types A and B); however, the effect of piezoresistor length is substantially reduced for type C and D. Cantilever type D has a greater base width than type B but the same overall length, leading to a comparative increase in lateral stiffness in that region; however, the transverse tapering towards the free end effectively reduces the lateral stiffness away from the clamped base.

By comparing all of the designs, we conclude that cantilevers which are long and narrow are better suited for point-loading applications such as AFM, which is consistent with published reports [9, 10].

To test the response of the cantilever designs to an applied surface stress, we use an approach based on the use of cantilevers as transducers in chemical vapor sensing. We have previously utilized polymer-coated cantilever arrays as sensors for volatile organic compounds [7], where the gas-phase molecules are reversibly absorbed into the

coatings; as they undergo volumetric strain, the well-adhered coatings impart a surface stress to their respective cantilevers, which bend in response. Since a standardized sensor response is critical for a meaningful assessment of the cantilever designs, coatings with a high uniformity of thickness and distribution across the test arrays are necessary; we have therefore elected to apply the same vapor sensing strategy to hydrogen gas detection using palladium (Pd) thin films, where simultaneous evaporative deposition of the Pd onto the test array of cantilevers ensures that they have practically identical coatings. Such films are known to reversibly absorb hydrogen and undergo substantial volumetric strain, and have been recently employed in several cantilever-based hydrogen sensors [17-20]

The cantilevers were mounted and wire-bonded as above (Fig. 6b). A custom flow cell seals the cantilevers into a chamber, allowing the test platform to interface with a hydrogen gas (H₂) manifold; the low-profile, low volume design provides laminar gas flow across the cantilevers (Fig. 6a). For each pair of identical levers, one cantilever was functionalized with 25 nm of Pd deposited by e-beam evaporation on the native silicon substrate under moderate vacuum ($1-2 \times 10^{-6}$ Torr); the remaining cantilever was masked to provide a coating-free reference (Fig. 7).

The Pd-functionalized cantilevers were exposed to ~2.5% H₂ in an argon (Ar) diluent flow; these ultrahigh purity (>99.999%) gases were obtained from Airgas (Radnor, PA, USA) and Air Liquide America (Countryside, IL, USA), respectively. Model 1179 Viton-sealed mass-flow controllers from MKS Instruments (Wilmington, MA, USA) were used to regulate the analyte and diluent gases at a total constant flow of 410 standard cubic centimeters per minute (sccm).

The cantilever response to hydrogen absorption was sampled from each functionalized cantilever with respect to the corresponding, bare reference cantilever (i.e., the differential deflection); this data acquisition strategy permits common-mode noise rejection. Wheatstone bridge circuits (one per cantilever) were used to measure the differential resistance changes as a function of time, and the resulting voltages were captured via data acquisition. A schematic diagram of the experimental test apparatus is shown in Fig. 8.

Figure 9 shows representative differential cantilever responses of the Pd-coated cantilevers to hydrogen. Maximum deflection responses, corresponding to equilibrium saturation of the sensor coatings, are shown in Fig. 10; since these voltage signals represent resistance changes in the piezoresistive cantilever, they provide a direct measurement of the sensitivity under mechanical load. We first examine the sensitivity of cantilever type E (narrow) versus type B (wide), which have equivalent piezoresistor lengths. For surface stress loading, type B has a sensitivity that is 5.3 times that of type E, a relationship that is nearly the opposite of that observed in the point-loading case. The type B design has a larger stress difference σ_{lt} near its base than the type E design under applied surface stress.

4. Discussion

To understand the relative behavior in the surface stress versus point loading cases, we must consider the relative role of the transverse contributions to the internal stress. Under surface stress loading, the lateral stresses do not dominate the mechanical behavior of the cantilever as in the intrinsically asymmetrical point-load case; in the

extreme, idealized case of an unclamped cantilever (i.e., a plate), the stress is in fact isotropic, and the lateral and transverse stresses are equivalent. The clamping of the cantilever at its base strongly restricts transverse deflection in this region, creating a disparity between the lateral and transverse stresses that diminishes towards the free end of the beam. Cantilever type E has half the width of type B, but the same length; therefore, it should have less transverse stiffness and thus a smaller average stress difference in the piezoresistive region at the clamped base than the type B design; the result is that type E exhibits less sensitivity than type B under surface stress loading, just as we have observed. These experimental results support the conclusion that cantilevers which are short and wide are better suited for surface stress loading scenarios such as those that occur in sensor applications.

For a given cantilever shape (square or trapezoidal), the design with the shorter, proportionate piezoresistor possesses the greater surface stress sensitivity; however, the enhancements observed here are much less significant than those found for the same designs under point loading. Cantilever type A ($L_p/L_c = 0.3$) has a slightly higher point-load sensitivity than type B ($L_p/L_c = 1.0$). A similar relationship is observed for the trapezoidal designs; cantilever type C ($L_p/L_c = 0.3$) has a slightly higher point-load sensitivity than type D ($L_p/L_c = 1.0$). For these geometries, the internal stress difference σ_{lt} varies much less from clamped base to free end than in the point-loading situation, at least in the case of the square cantilevers (types A and B).

Fig. 10 shows that the trapezoidal geometries (types C and D) behave more like the rectangular (type E) than the square (types A and B) designs under surface stress loading. The trapezoidal cantilevers (types C and D) are less sensitive than the square

cantilevers (types A and B) to surface stress, but are more sensitive than the rectangular cantilever (type E). For the trapezoidal cantilevers, a small piezoresistor at the base (type C) is more sensitive than a large piezoresistor that covers the entire cantilever (type D).

Overall, the results of this study provide experimental validation of previously published theoretical work on the design of piezoresistive cantilevers for biological and chemical sensing [12]. Piezoresistive cantilever response to a point load is qualitatively different than piezoresistive cantilever response to surface stress. In contrast to piezoresistive cantilevers optimized for probe microscopy, piezoresistive cantilevers for sensing are optimal when they are short and wide. The region of highest σ_{lt} is near the center of the cantilever base, and so for the cantilever designs considered here, the cantilever piezoresistors in this location are better for sensing than cantilevers with distributed piezoresistors.

5. Conclusions

We have designed, fabricated, and performed validation testing of five piezoresistive cantilever configurations to investigate the effect of shape and piezoresistor placement on the sensitivity of microcantilevers under both point and surface mechanical loading. High aspect ratio cantilevers are optimal for point-loading applications such as AFM or force measurements, and low aspect ratio cantilevers are better for surface stress loading scenarios such as those that occur in biological and chemical sensor applications. The sensitivity data for both point loads and surface stress are consistent with previously developed finite-element models.

Acknowledgement

This work was performed under the auspices of the U.S. Department of Energy by Lawrence Livermore National Laboratory under Contract DE-AC52-07NA27344. We thank D. Sirbuly and M. Stadermann for laboratory assistance.

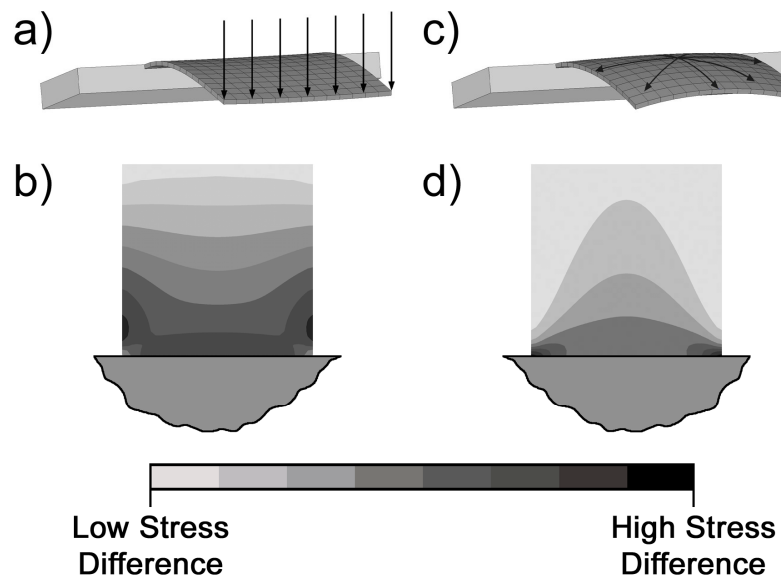


Fig. 1 Finite-element models of linear versus surface stress loading of a microcantilever (adapted from Ref. [12]). Mechanical deformation (top row) and corresponding spatial maps of lateral stress minus transverse stress (bottom row) for a line load applied at the free end (a and b) and a load applied across the entire surface (c and d).

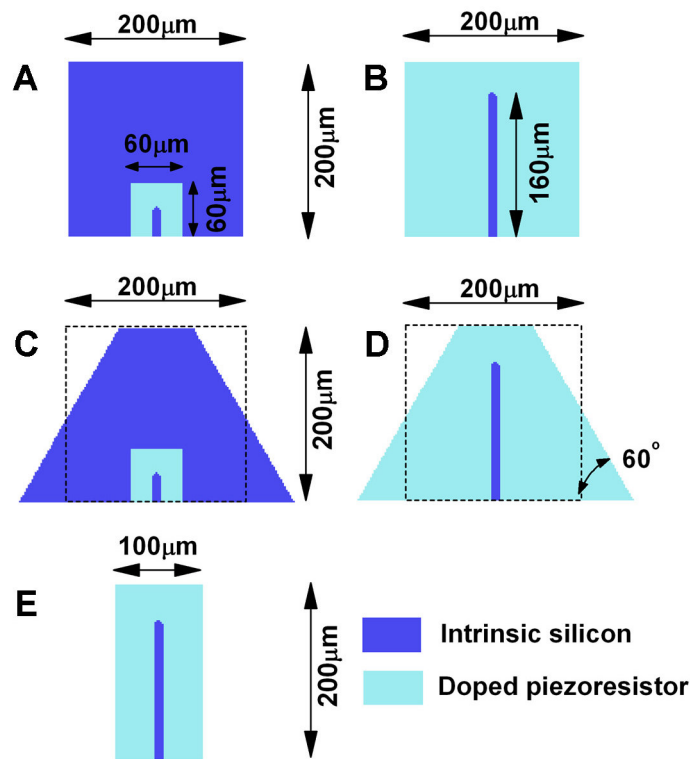


Fig. 2 Five cantilever designs (A-E) with different shapes and piezoresistor regions, designed to study the effect of geometrical parameters on surface stress sensitivity. Light blue areas indicate boron-doped piezoresistive regions, and dark blue areas indicate intrinsic silicon.

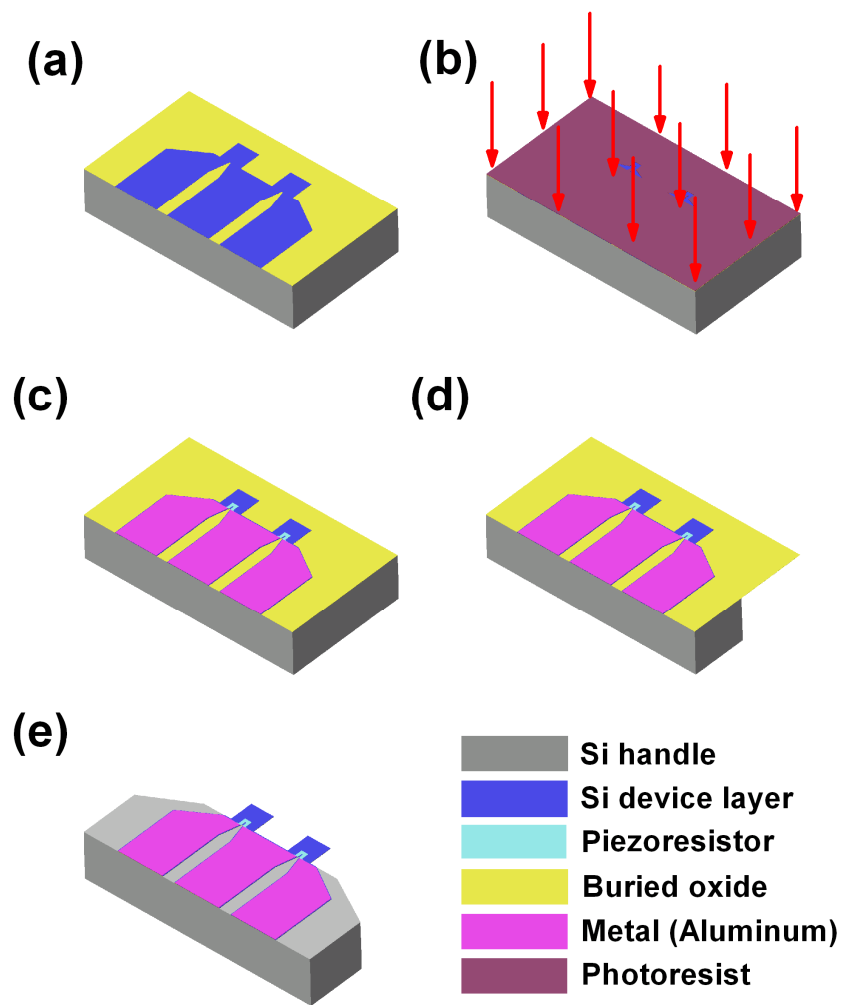


Fig. 3 Schematic of the five major fabrication steps: (a) cantilever structures are etched into the device layer; (b) boron doped piezoresistors are defined by ion implantation; (c) contacts are opened in the PECVD oxide layer, and metal is deposited in a liftoff process; (d) silicon handle layer is selectively etched from the backside; (e) buried oxide layer is removed with hydrofluoric acid.

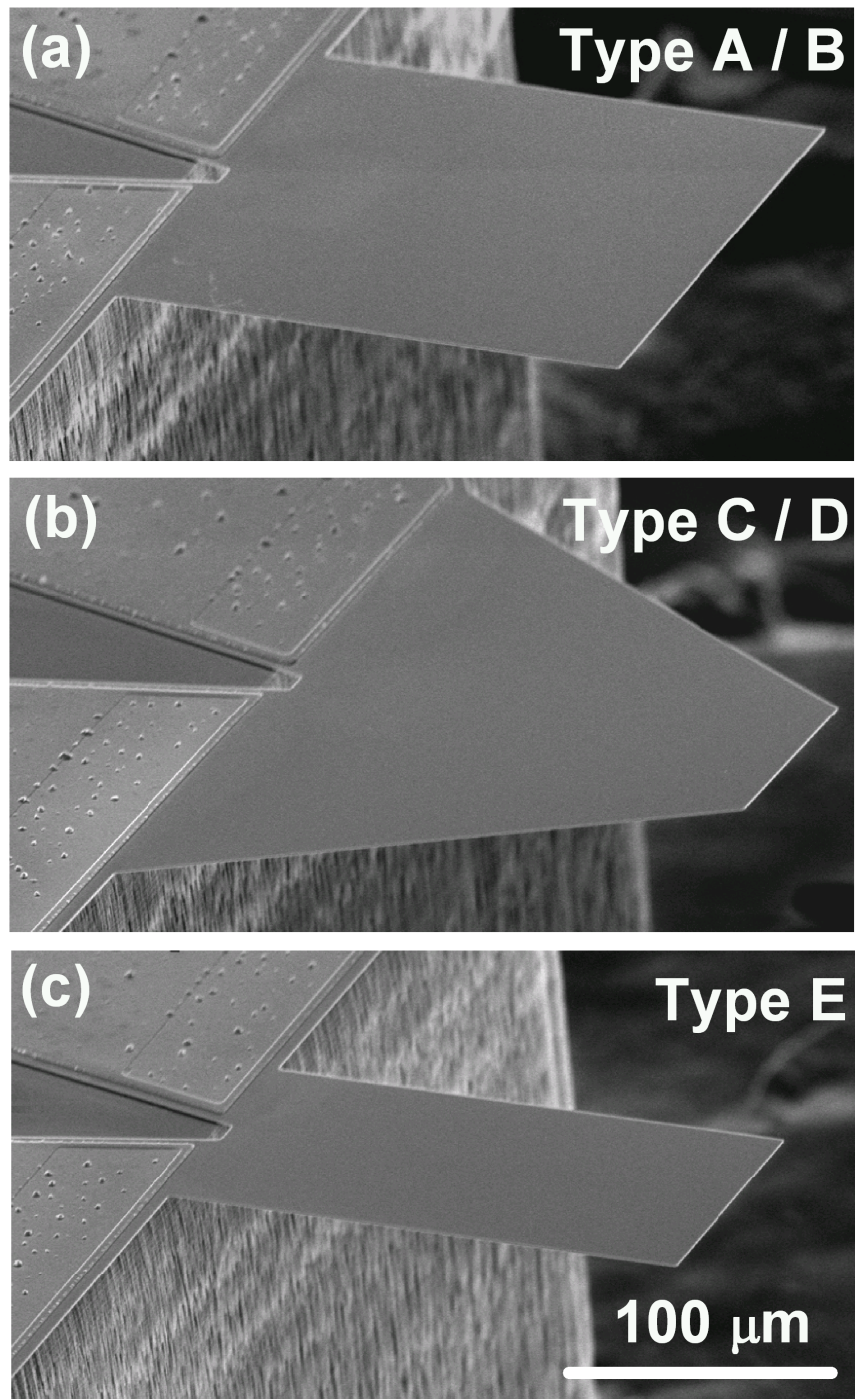


Fig. 4 Scanning electron micrographs of the released cantilevers. Note that the two square designs (types A and B) are mutually indistinguishable in external appearance; the two trapezoidal designs (types C and D) are also visually identical.

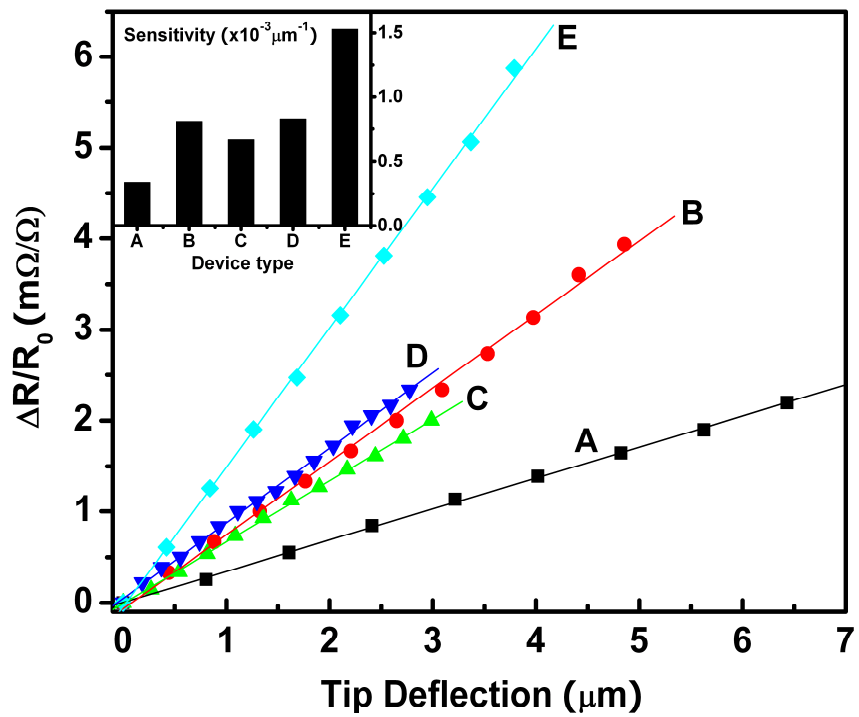


Fig. 5 Resistance versus tip deflection due to an applied point load for the five cantilever designs (A-E).

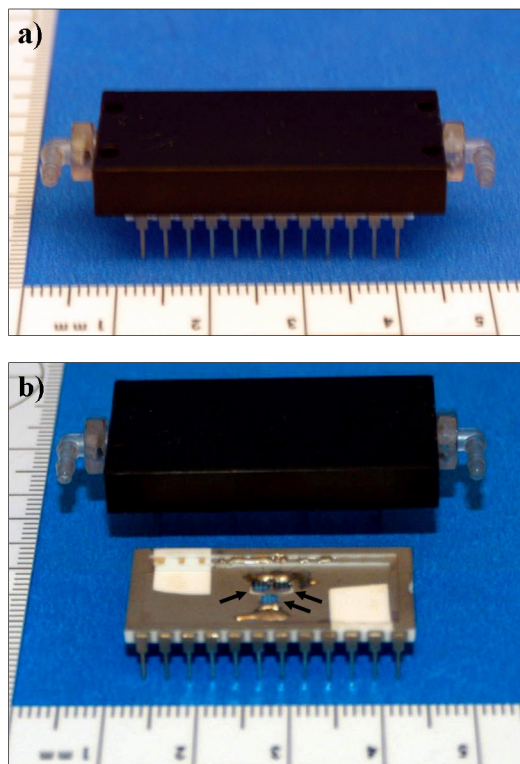


Fig. 6. Photographs of the DIP-mounted test array of piezoresistive cantilevers: a) with flow cell mounted; b) exploded view of flow cell and representative test array. Note the location of three silicon chips (*arrows*), each bearing a pair of identical cantilevers (Pd-coated and bare).

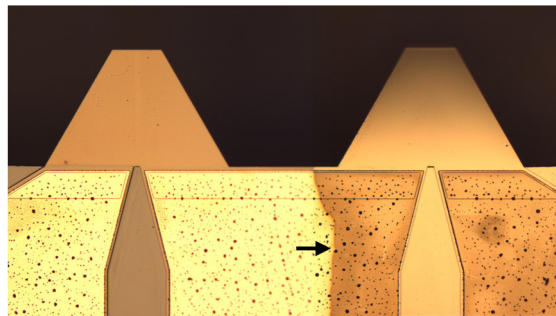


Fig. 7. Photomicrograph of Pd-functionalized (*right*) and bare reference (*left*) piezoresistive cantilevers of design type D. The rough vertical border near the center of the image (*arrow*) indicates the edge of the metal film delineated by the evaporation mask.

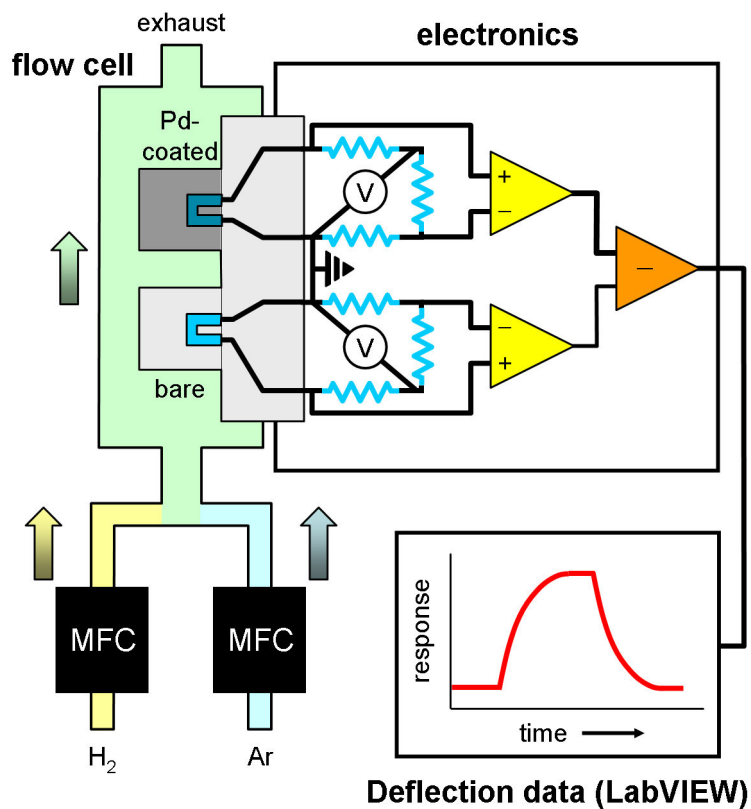


Fig. 8 Schematic of the experimental test apparatus. Pairs of each piezoresistive cantilever design (Pd-coated and bare) are exposed to the 2.5% H₂/Ar mixture, which is prepared using mass flow controllers (MFCs). The differential deflection response of the cantilever pair is measured by the electronics, and subsequently processed and read out using LabVIEW.

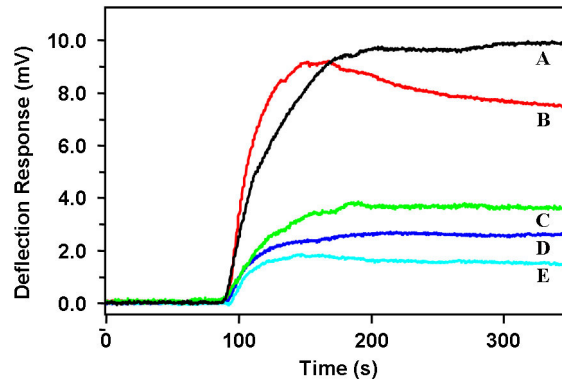


Fig. 9. Representative differential deflection response versus time of Pd-functionalized cantilevers (A-E) to 2.5% H₂/Ar mixture.

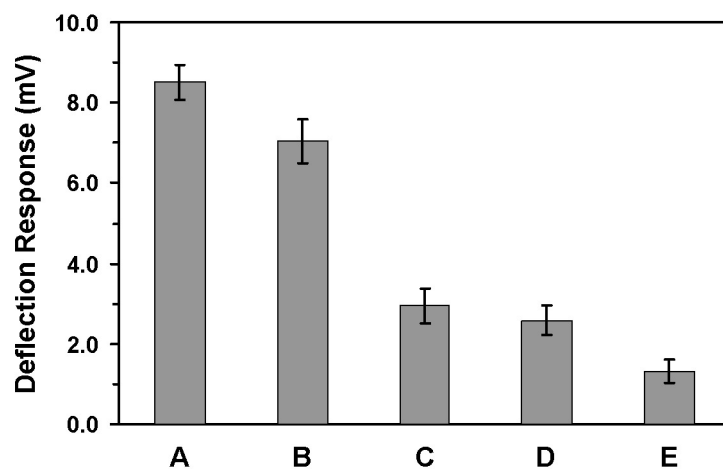


Fig. 10. Column plot of average deflection responses for the Pd-functionalized cantilever designs (A-E). Each column represents the maximum deflection to 3-5 serial H₂/Ar mixture exposures separated by Ar purges.

References

- [1] G. Y. Chen, T. Thundat, E. A. Wachter, and R. J. Warmack, "Adsorption-Induced Surface Stress and its Effects on Resonance Frequency of Microcantilevers," *Journal of Applied Physics*, vol. 77, pp. 3618-3622, Apr 1995.
- [2] H. J. Butt, "A sensitive method to measure changes in the surface stress of solids," *Journal of Colloid and Interface Science*, vol. 180, pp. 251-260, Jun 1996.
- [3] R. Berger, E. Delamarche, H. P. Lang, C. Gerber, J. K. Gimzewski, E. Meyer, and H. J. Guntherodt, "Surface stress in the self-assembly of alkanethiols on gold," *Science*, vol. 276, pp. 2021-2024, Jun 1997.
- [4] S. T. Koev, M. A. Powers, H. Yi, L. Q. Wu, W. E. Bentley, G. W. Rubloff, G. F. Payne, and R. Ghodssi, "Mechano-transduction of DNA hybridization and dopamine oxidation through electrodeposited chitosan network," *Lab on a Chip*, vol. 7, pp. 103-111, 2007.
- [5] V. Dauksaite, M. Lorentzen, F. Besenbacher, and J. Kjems, "Antibody-based protein detection using piezoresistive cantilever arrays," *Nanotechnology*, vol. 18, Mar 2007.
- [6] D. Then, A. Vidic, and C. Ziegler, "A highly sensitive self-oscillating cantilever array for the quantitative and qualitative analysis of organic vapor mixtures," *Sensors and Actuators B-Chemical*, vol. 117, pp. 1-9, Sep 12 2006.
- [7] A. Loui, T. V. Ratto, T. S. Wilson, S. K. McCall, E. V. Mukerjee, and B. R. Hart, "Chemical Vapor Discrimination Using a Compact and Low-Power Array of Piezoresistive Microcantilevers," *The Analyst*, vol. 133, pp. 608-615, May 2008.

- [8] M. Tortonese, H. Yamada, R. C. Barrett, and C. F. Quate, "Atomic force microscopy using a piezoresistive cantilever," in *Solid-State Sensors and Actuators, 1991. Digest of Technical Papers, TRANSDUCERS '91., 1991 International Conference on*, 1991, pp. 448-451.
- [9] J. A. Harley and T. W. Kenny, "High-sensitivity piezoresistive cantilevers under 1000 Å thick," *Applied Physics Letters*, vol. 75, pp. 289-291, 1999.
- [10] J. A. Harley and T. W. Kenny, "1/f noise considerations for the design and process optimization of piezoresistive cantilevers," *Microelectromechanical Systems, Journal of*, vol. 9, pp. 226-235, 2000.
- [11] P. A. Rasmussen, J. Thaysen, O. Hansen, S. C. Eriksen, and A. Boisen, "Optimised cantilever biosensor with piezoresistive read-out," *Ultramicroscopy*, vol. 97, pp. 371-376, Oct-Nov 2003.
- [12] F. T. Goericke and W. P. King, *IEEE Sensors Journal*, in press.
- [13] Y. Kanda, "A graphical representation of the piezoresistance coefficients in silicon," *Electron Devices, IEEE Transactions on*, vol. 29, pp. 64-70, 1982.
- [14] F. Goericke, J. Lee, and W. P. King, "Microcantilever hotplates with temperature-compensated piezoresistive strain sensors," *Sensors and Actuators A: Physical*, vol. 143, pp. 181-190, 2008.
- [15] J. Lee and W. P. King, "Microcantilever hotplates: Design, fabrication, and characterization," *Sensors and Actuators A: Physical*, vol. 136, pp. 291-298, 2007.
- [16] B. W. Chui, L. Aeschimann, T. Akiyama, U. Staufer, N. F. d. Rooij, J. Lee, F. Goericke, W. P. King, and P. Vettiger, "Advanced temperature compensation for

- piezoresistive sensors based on crystallographic orientation," *Review of Scientific Instruments*, vol. 78, p. 043706, 2007.
- [17] A. Fabre, E. Finot, J. Demoment, and S. Contreras, "Monitoring the chemical changes in Pd induced by hydrogen absorption using microcantilevers," *Ultramicroscopy*, vol. 97, pp. 425-432, Oct-Nov 2003.
- [18] D. R. Baselt, B. Fruhberger, E. Klaassen, S. Cemalovic, C. L. Britton, S. V. Patel, T. E. Mlsna, D. McCorkle, and B. Warmack, "Design and performance of a microcantilever-based hydrogen sensor," *Sensors and Actuators B-Chemical*, vol. 88, pp. 120-131, Jan 2003.
- [19] S. Okuyama, Y. Mitobe, K. Okuyama, and K. Matsushita, "Hydrogen gas sensing using a Pd-coated cantilever," *Japanese Journal of Applied Physics Part 1- Regular Papers Short Notes & Review Papers*, vol. 39, pp. 3584-3590, Jun 2000.
- [20] M. Tabib-Azar and S. R. LeClair, "Applications of evanescent microwave probes in gas and chemical sensors," *Sensors and Actuators B-Chemical*, vol. 67, pp. 112-121, Aug 2000.